

# Wavenumber selection for small–wavelength Görtler vortices in curved channel flows

Andrew Dando & Philip Hall

Department of Mathematics,  
Oxford Road,  
University of Manchester,  
Manchester, M13 9PL.  
United Kingdom.

## Abstract

We consider the problem of wavenumber selection for fully nonlinear, small–wavelength Görtler vortices in a curved channel flow. These type of Görtler vortices were first considered by Hall & Lakin (1988) for an external boundary layer flow. They proved particularly amenable to asymptotic description, it was possible to consider vortices large enough so that the mean flow correction driven by them is as large as the basic state, and this prompted us to consider them in a curved channel flow as an initial application of the phase–equation approach to Görtler vortices. This involves the assumption that the phase variable of these Görtler vortices varies on slow spanwise and time scales, then an analysis of both inside and outside the core region, to which vortex activity is restricted, leads to a system of partial differential equations which we can solve numerically for the wavenumber. We consider in particular the effect on the wavenumber of the outer channel wall varying on the same slow spanwise scale as the phase variable.

---

<sup>1</sup>This research was partially supported by the National Aeronautics and Space Administration under NASA Contract No. NAS1-19480 while the authors were in residence at the Institute for Computer Applications in Science and Engineering (ICASE), NASA Langley Research Center, Hampton, VA 23681-0001.

# 1 Introduction

Much innovative work was done during the 1980's on wavenumber selection, particularly for convection problems. Attention turned towards selection mechanisms that relied on the global physics and geometry of the system. The method developed is now referred to as the 'phase-equation' approach. Much of this work (see for instance Kramer et. al. 1982, Cross & Newell 1984, Buell & Catton 1986 and the review article by Newell, Passot & Lega 1993) was concerned with Rayleigh-Bénard convection problems although the ideas behind it had been encountered earlier in the context of travelling wave instabilities (Whitham 1974 and Howard & Kopell 1977).

Rayleigh-Bénard convection is a classical example for pattern forming transitions in nonequilibrium systems. The spatially uniform conducting state becomes unstable to spatially periodic time-independent rolls. The stability of these rolls had previously been studied by Galerkin techniques which suggested that for a range of Rayleigh numbers (dependent on the Prandtl number and wavenumber) these straight rolls are stable. However, in experiments large enough to contain many rolls these solutions were usually not seen. Instead more complicated patterns are common with curved rolls, roll dislocations and superimposed rolls present and sometimes time independent states are not even reached. The presence of these complicated patterns was attributed to factors such as the existence of orientational degeneracy, the observation that rolls tend to align themselves normal to lateral boundaries and the fact that there is a band of stable wavenumbers.

The 'phase-equation' approach did much to explain and predict the complicated patterns that are seen in experiments. For example, the dislocation of convection rolls is now fairly well understood using the phase equation approach. The phase-equation approach assumes that the phase is a function of slow (global) variables. All quantities are then expanded in terms of a suitable small parameter and substituted into the governing equations. At leading order the unmodulated equations of motion are recovered but at next order a linearised inhomogeneous form of the leading order problem is obtained. In order for this inhomogeneous problem to have a non-trivial solution a solvability condition must be satisfied and it is this solvability condition which gives an equation for the phase.

Recently these 'phase-equation' ideas have begun to be applied to boundary layer problems. Hall (1994) has used the phase-equation methods to consider large amplitude Tollmien-Schlichting waves in boundary layer flows. He considered asymptotically both large Reynolds number flows and finite Reynolds number flows (for the asymptotic suction profile). The results suggest that for both large and finite Reynolds numbers a uniform wavetrain of Tollmien-Schlichting waves will break down with either a singularity or a shock developing after a finite time. Here we shall use these phase-equation ideas to consider wavenumber selection for small-wavelength Görtler vortices in a curved channel flow.

Hall (1982) considered weakly nonlinear small-wavelength Görtler vortices, in an external boundary layer flow, and showed that this nonlinear interaction is not described by the Stuart-Watson approach. Hall & Lakin (1988) followed up this work by looking at the fully nonlinear interaction and they found that in the region of vortex activity the boundary layer flow is being

forced by the vortex which is in turn driven by the boundary layer. Surprisingly they also found that an asymptotic description could be obtained for this nonlinear interaction when the vortices are of sufficient size that the mean flow correction driven by them is as large as the basic state. This amenability to asymptotic description was one of the main reasons for making an initial phase–equation study on this type of Görtler vortices.

In the next section we shall consider the formulation of our problem. From the previous work of Hall & Lakin (1988) and Bassom (1989) we know that the vortices will be contained within a core region. In §3 we consider asymptotically the flow within this core region. In §4 we match the solutions from inside and outside the core region. In the process we derive a system of partial differential equations involving the wavenumber. Then in §5 we consider numerical solutions of the equations we have derived for a variety of different geometries for the outer channel wall. Finally in §6 we draw some conclusions from our numerical results and consider how far we have progressed in providing a theoretical explanation for the non–uniform patterns of vortices frequently observed in experiments (see Swearingen & Blackwelder 1987 and references therein) and also in computational studies (Guo & Finlay 1994).

## 2 Formulation of the Governing Equations

In this work we consider the flow of an incompressible viscous fluid of density  $\rho$  and kinematic viscosity  $\nu$  in a curved channel. The walls of the channel, with respect to the usual cylindrical polar co–ordinates  $(r', \theta', z')$ , are given by  $r' = R$  and  $r' = R + dq(\tilde{z})$  where  $d$  is a typical gap width (see the next section for a discussion of the slow spanwise scale,  $\tilde{z} = \epsilon^{\frac{7}{2}}z$ , on which the function  $q$  varies). The non–dimensional co–ordinates  $(x, y, z)$  are defined by

$$x = \frac{1}{Re} \frac{R\theta'}{d} \quad , \quad y = \frac{r' - R}{d} \quad , \quad z = \frac{z'}{d} \quad , \quad (2.1a, b, c)$$

where the Reynolds number  $Re = V_a d / \nu$  and  $V_a$  is the maximum azimuthal flow velocity.

The basic velocity and pressure fields for this small gap limit ( $\delta = d/R \ll 1$ ) take the form

$$(\hat{u}, \hat{v}, \hat{w}) = V_a(u, Re^{-1}v, Re^{-1}w) + O(\delta V_a) \quad , \quad \hat{p} = p \quad , \quad (2.2)$$

and we confine our attention to the limit  $Re \rightarrow \infty$  with the Görtler number  $G$  defined by

$$G = Re^2 \delta = \frac{V_a^2 d^3}{R\nu^2} \quad , \quad (2.3)$$

held fixed. We find that the Navier–Stokes equations for this problem are

$$\frac{\partial u}{\partial x} + \frac{\partial v}{\partial y} + \frac{\partial w}{\partial z} = 0 \quad , \quad (2.4a)$$

$$\frac{\partial^2 u}{\partial y^2} + \frac{\partial^2 u}{\partial z^2} - \frac{\partial u}{\partial t} - \frac{\partial p}{\partial x} = u \frac{\partial u}{\partial x} + v \frac{\partial u}{\partial y} + w \frac{\partial u}{\partial z} \quad , \quad (2.4b)$$

$$\frac{\partial^2 v}{\partial y^2} + \frac{\partial^2 v}{\partial z^2} - \frac{\partial v}{\partial t} - \frac{1}{2}Gu^2 - \frac{\partial p}{\partial y} = u \frac{\partial v}{\partial x} + v \frac{\partial v}{\partial y} + w \frac{\partial v}{\partial z} \quad , \quad (2.4c)$$

$$\frac{\partial^2 w}{\partial y^2} + \frac{\partial^2 w}{\partial z^2} - \frac{\partial w}{\partial t} - \frac{\partial p}{\partial z} = u \frac{\partial w}{\partial x} + v \frac{\partial w}{\partial y} + w \frac{\partial w}{\partial z} \quad . \quad (2.4d)$$

We choose to concentrate on vortices with small,  $O(\epsilon)$ , wavelengths. Previous work has shown that such vortices exist at large,  $O(\epsilon^{-4})$ , Görtler numbers. So we expand the Görtler number for this flow as

$$G = \epsilon^{-4}(G_0 + \epsilon G_1 + \dots) \quad , \quad (2.5)$$

and the mean flow quantities as

$$(u, v, w) = (\bar{u}(y, \tilde{z}, \tilde{t}), \epsilon^3 \bar{v}(y, \tilde{z}, \tilde{t}), \epsilon^{-\frac{1}{2}} \bar{w}(y, \tilde{z}, \tilde{t}))$$

$$p = -2F(\tilde{z}, \tilde{t})x + \epsilon^{-4} \bar{p}(y, \tilde{z}, \tilde{t}) \quad . \quad (2.6)$$

Again, see the next section for a discussion of the slow timescale,  $\tilde{t} = \epsilon^3 t$ . We find that vortex activity is restricted to a core region and outside of this core substitution of (2.6) into the governing equations, (2.4a-d), gives

$$\frac{\partial \bar{v}}{\partial y} = -\frac{\partial \bar{w}}{\partial \tilde{z}} \quad , \quad (2.7a)$$

$$\frac{\partial^2 \bar{u}}{\partial y^2} = -2F \quad , \quad (2.7b)$$

$$-\frac{1}{2}G_0 \bar{u}^2 = \frac{\partial \bar{p}}{\partial y} \quad , \quad (2.7c)$$

$$\frac{\partial^2 \bar{w}}{\partial y^2} = \frac{\partial \bar{p}}{\partial \tilde{z}} \quad , \quad (2.7d)$$

subject to the boundary conditions

$$\bar{u} = \bar{v} = \bar{w} = 0 \quad \text{at} \quad y = 0, q \quad . \quad (2.8)$$

### 3 Derivation of the Nonlinear Equations for Görtler Vortices in Curved Channel Flow

We now develop an asymptotic solution of the governing equations valid in the presence of vortices which have small wavelengths. The previous work of Hall(1982), Hall & Lakin (1988) and Bassom (1989) suggests that the vortices will be contained within a core region. The flowfield is therefore split up as shown in Figure 1 with the vortex activity confined to the region between  $y_1$  and  $y_2$ . The layers denoted by regions IIa,b are transition layers, of width

$O(\epsilon^{\frac{2}{3}})$ , required to smooth out the algebraically decaying vortices in region I. In region I the appropriate expansions of  $u$ ,  $v$ ,  $w$  and  $p$  are

$$u = \bar{u}_0 + \epsilon^{\frac{1}{2}}\bar{u}_1 + \epsilon\bar{u}_2 + \cdots + \left[ \epsilon(U_0E + c.c.) + \epsilon^{\frac{3}{2}}(U_1E + c.c.) + \epsilon^2(U_2E + c.c.) + \cdots \right] + \cdots \quad , \quad (3.1a)$$

$$v = \epsilon^3\bar{v}_0 + \epsilon^{\frac{7}{2}}\bar{v}_1 + \epsilon^4\bar{v}_2 + \cdots + \left[ \epsilon^{-1}(V_0E + c.c.) + \epsilon^{-\frac{1}{2}}(V_1E + c.c.) + (V_2E + c.c.) + \cdots \right] + \cdots \quad , \quad (3.1b)$$

$$w = \epsilon^{-\frac{1}{2}}\bar{w}_0 + \bar{w}_1 + \epsilon^{\frac{1}{2}}\bar{w}_2 + \cdots + \left[ (W_0E + c.c.) + \epsilon^{\frac{1}{2}}(W_1E + c.c.) + \epsilon(W_2E + c.c.) + \cdots \right] + \cdots \quad , \quad (3.1c)$$

$$p = -2Fx + \epsilon^{-4}\bar{p}_0 + \epsilon^{-\frac{7}{2}}\bar{p}_1 + \epsilon^{-3}\bar{p}_2 + \cdots \\ + \left[ \epsilon^{-1}(P_0E + c.c.) + \epsilon^{-\frac{1}{2}}(P_1E + c.c.) + (P_2E + c.c.) + \cdots \right] + \cdots \quad . \quad (3.1d)$$

Mean flow terms (apart from the pressure gradient  $F$ ) are denoted by barred small letters and vortex terms by capital letters. We assume that the mean flow quantities and disturbances are all independent of  $x$  and the notation  $c.c.$  denotes the complex conjugate, whilst the exponential  $E$  is given by

$$E = \exp\left\{ \frac{i}{\epsilon^{\frac{3}{2}}}\theta(\tilde{z}, \tilde{t}) \right\} \quad , \quad (3.2)$$

where

$$\tilde{z} = \epsilon^{\frac{7}{2}}z \quad , \quad \tilde{t} = \epsilon^3t \quad , \quad (3.3)$$

and  $\theta$  is a phase variable. The slow  $z$ -scale is determined by our requirement that  $\partial/\partial z \sim \epsilon^{-1}$  and also by balancing terms in the mean flow  $z$ -momentum equation. In this paper we have, for convenience, fixed our attention on  $\tilde{z} = \epsilon^{\frac{7}{2}}z$  although we could have considered  $\tilde{z} = \epsilon^k z$  where  $3 < k < 4$ . Hall (1985) showed, in contrast to the two-dimensional case, that the Görtler disturbances applied to a three-dimensional flow are necessarily time dependent and hence the inclusion of this slow time-scale which is necessary to provide a term for the consistency condition at the second order of the fundamental equations (equation 3.13a). We write  $\Theta = i\epsilon^{-\frac{3}{2}}\theta(\tilde{z}, \tilde{t})$  so that  $\partial/\partial z \rightarrow ik\epsilon^{-1}\partial/\partial\Theta$  and  $\partial/\partial t \rightarrow -i\Omega\epsilon^{-\frac{3}{2}}\partial/\partial\Theta$  where the wavenumber  $k = \theta_{\tilde{z}}$  and the frequency  $\Omega = -\theta_{\tilde{t}}$ . The introduction of the wavenumber and frequency imply that we must have a phase conservation equation, namely

$$\frac{\partial k}{\partial \tilde{t}} + \frac{\partial \Omega}{\partial \tilde{z}} = 0 \quad . \quad (3.4)$$

Strictly, higher harmonics are also present in the expansions (3.1), but they do not affect our calculation at the orders we shall be concerned with.

Substituting the expansions (3.1) into the governing equations we find that the leading order fundamental equations give

$$V_{0y} + ikW_0 = 0 \quad , \quad (3.5a)$$

$$k^2U_0 + \bar{u}_{0y}V_0 = 0 \quad , \quad (3.5b)$$

$$k^2V_0 + G_0\bar{u}_0U_0 = 0 \quad , \quad (3.5c)$$

$$k^2 W_0 + ikP_0 = 0 \quad , \quad (3.5d)$$

and consistency of (3.5b) and (3.5c) implies that throughout the core

$$G_0 \bar{u}_0 \bar{u}_{0y} = k^4 \quad , \quad (3.6a)$$

from which we can see that

$$\bar{u}_0 = \frac{(2k^4 y + a(\tilde{z}, \tilde{t}))^{\frac{1}{2}}}{G_0^{\frac{1}{2}}} \quad , \quad (3.6b)$$

where  $a$  is an, as yet undetermined, arbitrary function of  $\tilde{z}$  and  $\tilde{t}$ . At the leading order of the mean flow we find that the governing equations give

$$\bar{v}_{0y} + \bar{w}_{0z} = 0 \quad , \quad (3.7a)$$

$$\bar{u}_{0yy} + 2F = V_0 \bar{U}_{0y} + \bar{V}_0 U_{0y} + ikU_0 \bar{W}_0 - ik\bar{U}_0 W_0 \quad , \quad (3.7b)$$

$$\frac{1}{2} G_0 \bar{u}_0^2 + \bar{p}_{0y} = 0 \quad , \quad (3.7c)$$

$$0 = V_0 \bar{W}_{0y} + \bar{V}_0 W_{0y} \quad , \quad (3.7d)$$

where we have used a bar on the capital (vortex) terms to denote the complex conjugate of this quantity. Using (3.5) to substitute in for  $U_0$  and  $W_0$  we find that (3.7b,d) give

$$\bar{u}_{0yy} + 2F = -\frac{2}{k^2} \frac{\partial}{\partial y} \left( \bar{u}_{0y} V_0 \bar{V}_0 \right) \quad , \quad (3.8a)$$

$$0 = \frac{\partial}{\partial y} \left( V_0 \bar{V}_{0y} - \bar{V}_0 V_{0y} \right) \quad , \quad (3.8b)$$

and these two equations define the vortex function  $V_0$ . From (3.7c) we have

$$\bar{p}_{0y} = -\frac{1}{2} (2k^4 y + a) \quad , \quad (3.9a)$$

and after integration with respect to  $y$  we have

$$\bar{p}_0 = -\frac{1}{2} (k^4 y^2 + ay + c(\tilde{z}, \tilde{t})) \quad . \quad (3.9b)$$

The size of the vortex function  $V_0$  is now determined by integrating (3.8a) to give

$$\bar{u}_{0y} + 2Fy + B(\tilde{z}) = -\frac{2}{k^2} \bar{u}_{0y} |V_0|^2 \quad . \quad (3.10)$$

The function  $|V_0|^2$  cannot be negative so  $y_1$  and  $y_2$ , which determine the edges of region I, must satisfy (3.10) with  $V_0 = 0$ . If we then eliminate  $B(\tilde{z})$  from the resulting two equations we obtain the condition

$$\frac{k^4}{G_0^{\frac{1}{2}} (2k^4 y_1 + a)^{\frac{1}{2}}} + 2Fy_1 = \frac{k^4}{G_0^{\frac{1}{2}} (2k^4 y_2 + a)^{\frac{1}{2}}} + 2Fy_2 \quad . \quad (3.11)$$

This equation is obviously not sufficient to determine  $a$ ,  $y_1$  and  $y_2$  so we are not yet able to determine the location of the layers IIa,b.

At second order the fundamental equations give

$$V_{1y} + ikW_1 = 0 \quad , \quad (3.12a)$$

$$k^2U_1 + \bar{u}_{0y}V_1 = -\bar{u}_{1y}V_0 - i(-\Omega + \bar{w}_0k)U_0 \quad , \quad (3.12b)$$

$$k^2V_1 + G_0\bar{u}_0U_1 = -G_0\bar{u}_1U_0 - i(-\Omega + \bar{w}_0k)V_0 \quad , \quad (3.12c)$$

$$k^2W_1 + ikP_1 = -i(-\Omega + \bar{w}_0k)W_0 \quad , \quad (3.12d)$$

and consistency of (3.12b) and (3.12c) requires firstly that

$$-\Omega + \bar{w}_0k = 0 \quad , \quad (3.13a)$$

and secondly that

$$\frac{\partial}{\partial y}(\bar{u}_0\bar{u}_1) = 0 \quad . \quad (3.13b)$$

Equation (3.13b), as we expect, defines the second order component of the streamwise mean flow whilst (3.13a) provides an equation for the leading order component of the spanwise mean flow. Note also that, since  $\Omega$  and  $k$  are not functions of  $y$ , equation (3.13a) implies that  $\bar{w}_{0y} = 0$ .

We now need to determine the positions of the transition layers, IIa,b. The thickness of these layers is determined by a balance between diffusion across the layers and convection in the streamwise direction. This balance shows the layers to be  $O(\epsilon^{\frac{2}{3}})$  in depth and so we define in region IIa the  $O(1)$  variable

$$\xi = \frac{(y - y_2)}{\epsilon^{\frac{2}{3}}} \quad . \quad (3.14)$$

We are led to make the expansions

$$u = (\bar{u}_{00} + \epsilon^{\frac{2}{3}}\bar{u}_{01} + \epsilon^{\frac{4}{3}}\bar{u}_{02} + \dots) + \epsilon^{\frac{1}{2}}(\bar{u}_{10} + \epsilon^{\frac{2}{3}}\bar{u}_{11} + \epsilon^{\frac{4}{3}}\bar{u}_{12} + \dots) + \dots \\ + \{\epsilon^{\frac{4}{3}}(EU_{10} + c.c.) + \epsilon^2(EU_{11} + c.c.) + \dots\} + \dots \quad , \quad (3.15a)$$

$$v = \epsilon^3(\bar{v}_{00} + \epsilon^{\frac{2}{3}}\bar{v}_{01} + \epsilon^{\frac{4}{3}}\bar{v}_{02} + \dots) + \epsilon^{\frac{7}{2}}(\bar{v}_{10} + \epsilon^{\frac{2}{3}}\bar{v}_{11} + \epsilon^{\frac{4}{3}}\bar{v}_{12} + \dots) + \dots \\ + \{\epsilon^{-\frac{2}{3}}(EV_{10} + c.c.) + (EV_{11} + c.c.) + \dots\} + \dots \quad , \quad (3.15b)$$

$$w = \epsilon^{-\frac{1}{2}}(\bar{w}_{00} + \epsilon^{\frac{2}{3}}\bar{w}_{01} + \epsilon^{\frac{4}{3}}\bar{w}_{02} + \dots) + (\bar{w}_{10} + \epsilon^{\frac{2}{3}}\bar{w}_{11} + \epsilon^{\frac{4}{3}}\bar{w}_{12} + \dots) + \dots \\ + \{\epsilon^{-\frac{4}{3}}(EW_{10} + c.c.) + \epsilon^{-\frac{2}{3}}(EW_{11} + c.c.) + \dots\} + \dots \quad , \quad (3.15c)$$

$$p = -2Fx + \epsilon^{-4}(\bar{p}_{00} + \epsilon^{\frac{2}{3}}\bar{p}_{01} + \epsilon^{\frac{4}{3}}\bar{p}_{02} + \dots) + \epsilon^{-\frac{7}{2}}(\bar{p}_{10} + \epsilon^{\frac{2}{3}}\bar{p}_{11} + \epsilon^{\frac{4}{3}}\bar{p}_{12} + \dots) + \dots \\ + \{\epsilon^{-\frac{4}{3}}(EP_{10} + c.c.) + \epsilon^{-\frac{2}{3}}(EP_{11} + c.c.) + \dots\} + \dots \quad , \quad (3.15d)$$

in this layer because we can see from (3.10) that  $|V_0|^2 \sim y_2 - y$  when  $y \rightarrow y_{2-}$ .

Considering the solution of the governing equations in this layer we find that the fundamental x- and y-momentum equations give at  $O(\epsilon^{-\frac{2}{3}})$  and  $O(\epsilon^{-\frac{8}{3}})$  respectively

$$k^2 U_{10} + V_{10} \frac{\partial \bar{u}_{01}}{\partial \xi} = 0 \quad , \quad (3.16a)$$

$$k^2 V_{10} + G_0 \bar{u}_{00} U_{10} = 0 \quad , \quad (3.16b)$$

whilst at  $O(1)$  and  $O(\epsilon^{-2})$  of the same equations we obtain

$$k^2 U_{11} + V_{11} \frac{\partial \bar{u}_{01}}{\partial \xi} = \frac{\partial^2 U_{10}}{\partial \xi^2} - V_{10} \frac{\partial \bar{u}_{02}}{\partial \xi} \quad , \quad (3.17a)$$

$$k^2 V_{11} + G_0 \bar{u}_{00} U_{11} = 2 \frac{\partial^2 V_{10}}{\partial \xi^2} - G_0 \bar{u}_{01} U_{10} \quad . \quad (3.17b)$$

Equations (3.16a,b) are always consistent but for (3.17a,b) to be consistent we require that

$$3k^2 \frac{\partial^2 V_{10}}{\partial \xi^2} + k^4 \frac{\bar{u}_{01}}{\bar{u}_{00}} V_{10} + G_0 \bar{u}_{00} \frac{\partial \bar{u}_{02}}{\partial \xi} V_{10} = 0 \quad . \quad (3.18)$$

Looking at the mean flow x-momentum equation we find that at  $O(\epsilon^{-\frac{4}{3}})$ ,  $O(\epsilon^{-\frac{2}{3}})$  and  $O(1)$

$$\frac{\partial^2 \bar{u}_{00}}{\partial \xi^2} = 0 \quad , \quad (3.19a)$$

$$\frac{\partial^2 \bar{u}_{01}}{\partial \xi^2} = 0 \quad , \quad (3.19b)$$

$$\frac{\partial^2 \bar{u}_{02}}{\partial \xi^2} + 2F = V_{10} \frac{\partial \bar{U}_{10}}{\partial \xi} + \bar{V}_{10} \frac{\partial U_{10}}{\partial \xi} + ik \bar{W}_{10} U_{10} - ik W_{10} \bar{U}_{10} \quad . \quad (3.19c)$$

The solutions of (3.19a) and (3.19b) which match with the solutions in the core are

$$\bar{u}_{00} = \frac{(2k^4 y_2 + a)^{\frac{1}{2}}}{G_0^{\frac{1}{2}}} \quad , \quad (3.20a)$$

and

$$\bar{u}_{01} = \frac{k^4 \xi}{G_0^{\frac{1}{2}} (2k^4 y_2 + a)^{\frac{1}{2}}} \quad , \quad (3.20b)$$

whilst we find from (3.19c), after using the fundamental continuity and x-momentum equations to substitute in for  $U_{10}$  and  $W_{10}$ , that

$$\frac{\partial^2 \bar{u}_{02}}{\partial \xi^2} = -2F - \frac{2k^2}{G_0^{\frac{1}{2}} (2k^4 y_2 + a)^{\frac{1}{2}}} \frac{\partial |V_{10}|^2}{\partial \xi} \quad , \quad (3.21a)$$

and integrating this with respect to  $\xi$  gives

$$\frac{\partial \bar{u}_{02}}{\partial \xi} = -2F\xi - \frac{2k^2|V_{10}|^2}{G_0^{\frac{1}{2}}(2k^4y_2 + a)^{\frac{1}{2}}} + f(\tilde{z}) \quad , \quad (3.21b)$$

where  $f$  is an arbitrary function of  $\tilde{z}$  and  $\tilde{t}$  which we do not need to know explicitly for our purposes. If we now substitute (3.21b) back into equation (3.18) we find that

$$\frac{\partial^2 V_{10}}{\partial \xi^2} + \xi S(\tilde{z}, \tilde{t})V_{10} = \frac{2}{3}|V_{10}|^2V_{10} + g(\tilde{z}, \tilde{t})V_{10} \quad , \quad (3.22)$$

where

$$S(\tilde{z}, \tilde{t}) = \left[ \frac{k^6}{3(2k^4y_2 + a)} - \frac{2FG_0^{\frac{1}{2}}(2k^4y_2 + a)^{\frac{1}{2}}}{3k^2} \right] \quad , \quad (3.23a)$$

$$g(\tilde{z}, \tilde{t}) = -\frac{G_0^{\frac{1}{2}}(2k^4y_2 + a)^{\frac{1}{2}}}{3k^2} f \quad . \quad (3.23b)$$

Equation (3.22) is a particular form of the second Painlevé transcendent and has been shown by Hastings & McLeod (1980) to have a solution such that

$$S\xi \rightarrow \frac{2}{3}|V_{01}|^2 \quad \text{as} \quad \xi \rightarrow -\infty \quad , \quad |V_{01}| \rightarrow 0 \quad \text{as} \quad \xi \rightarrow +\infty \quad . \quad (3.24)$$

It follows that in layer IIa the fundamental terms decay to zero so that the finite amplitude Görtler vortex is trapped above region IIIa. We note that a similar analysis for the higher harmonics shows that these functions also decay exponentially to zero in IIa. However, the mean flow is virtually unaltered by the presence of IIa, thus the early terms in the expansions of the mean flow quantities in region IIa are simply obtained by expanding the mean flow in region I in terms of  $\xi$ . This means that the mean flow in region IIIa must to zeroth order when  $y \rightarrow y_{2+}$  have  $\bar{u}$ ,  $\bar{u}_y$ ,  $\bar{v}$ ,  $\bar{w}$ ,  $\bar{w}_y$  and  $\bar{p}$  defined by the coreflow solution evaluated with  $y = y_2$ .

An identical analysis can be carried out in region IIb with similar results. Hence in both region IIIa and IIIb there is only a mean velocity field. Therefore in the regions  $(0, y_1)$  and  $(y_2, q)$  the equations (2.7a-d) hold and we must solve them subject to the boundary conditions (2.8) and the matching conditions

$$\bar{u}(y_i) = \frac{(2k^4y_i + a)^{\frac{1}{2}}}{G_0^{\frac{1}{2}}} \quad , \quad \bar{u}_y(y_i) = \frac{k^4}{G_0^{\frac{1}{2}}(2k^4y_i + a)^{\frac{1}{2}}} \quad , \quad (3.25a, b)$$

$$\bar{w}(y_i) = \Omega/k \quad , \quad \bar{w}_y(y_i) = 0 \quad , \quad (3.25c, d)$$

$$\bar{v}(y_i) = -y_i(\Omega/k)\tilde{z} + b \quad , \quad (3.25e)$$

$$\bar{p}(y_i) = -\frac{1}{2}(k^4y_i^2 + ay_i + c) \quad , \quad i = 1, 2 \quad , \quad (3.25f)$$

along with the relationship between the positions  $y_1$  and  $y_2$  (equation 3.11).

## 4 Derivation of the Vortex Wavenumber Evolution Equation

Above the core, in region IIIb, equation (2.7b) gives

$$\frac{\partial^2 \bar{u}}{\partial y^2} = -2F(\tilde{z}, \tilde{t}) \quad , \quad (4.1)$$

and integrating this twice with respect to  $y$  gives, after we have applied the boundary condition  $\bar{u} = 0$  at  $y = 0$ ,

$$\bar{u} = y(A - yF) \quad , \quad (4.2)$$

where  $A$  is an as yet undetermined arbitrary function of  $\tilde{z}$  and  $\tilde{t}$ . Matching  $\bar{u}$  and  $\bar{u}_y$  at  $y_1$  (see equations 3.25a,b) implies that

$$k^4 = G_0 y_1 (A - y_1 F)(A - 2y_1 F) \quad , \quad (4.3)$$

$$a = -G_0 y_1^2 (A - y_1 F)(A - 3y_1 F) \quad . \quad (4.4)$$

Below the core equation (2.7b) again holds and integrating twice gives

$$\bar{u} = -Fy^2 + \bar{a}y + \bar{b} \quad ,$$

whilst matching  $\bar{u}$  and  $\bar{u}_y$  at  $y_2$  we find

$$\bar{a} = \frac{y_1^{\frac{1}{2}}(A - y_1 F)^{\frac{1}{2}}(A - 2y_1 F)}{[2y_2(A - 2y_1 F) - y_1(A - 3y_1 F)]^{\frac{1}{2}}} + 2Fy_2 \quad (4.5)$$

$$\begin{aligned} \bar{b} = -Fy_2^2 - \frac{y_2 y_1^{\frac{1}{2}}(A - y_1 F)^{\frac{1}{2}}(A - 2y_1 F)}{[2y_2(A - 2y_1 F) - y_1(A - 3y_1 F)]^{\frac{1}{2}}} \\ + y_1^{\frac{1}{2}}(A - y_1 F)^{\frac{1}{2}}[2y_2(A - 2y_1 F) - y_1(A - 3y_1 F)]^{\frac{1}{2}} \quad . \end{aligned} \quad (4.6)$$

We must satisfy the boundary condition  $\bar{u} = 0$  at  $y = q$  and this implies that

$$0 = -Fq^2 + \bar{a}q + \bar{b} \quad , \quad (4.7)$$

and upon substituting in for  $\bar{a}$  and  $\bar{b}$  we have

$$\begin{aligned} 0 = -F(q - y_2)^2 + \frac{(q - y_2)y_1^{\frac{1}{2}}(A - y_1 F)^{\frac{1}{2}}(A - 2y_1 F)}{[2y_2(A - 2y_1 F) - y_1(A - 3y_1 F)]^{\frac{1}{2}}} \\ + y_1^{\frac{1}{2}}(A - y_1 F)^{\frac{1}{2}}[2y_2(A - 2y_1 F) - y_1(A - 3y_1 F)]^{\frac{1}{2}} \quad . \end{aligned} \quad (4.8)$$

From our working inside the core we have equation (3.11), the relationship between the positions  $y_1$  and  $y_2$ , and after substituting in for  $k^4$  and  $a$ , using equations (4.3) and (4.4), this becomes

$$(A - 2y_2F) = \frac{y_1^{\frac{1}{2}}(A - y_1F)^{\frac{1}{2}}(A - 2y_1F)}{[2y_2(A - 2y_1F) - y_1(A - 3y_1F)]^{\frac{1}{2}}} \quad . \quad (4.9)$$

We now have three equations (4.3, 4.8 and 4.9) with which we can determine  $A$ ,  $y_1$  and  $y_2$  in terms of  $k$  and  $F$  (assuming we know  $G_0$  and  $q$ ).

Above the core the  $y$ -momentum equation is

$$\frac{\partial \bar{p}}{\partial y} = -\frac{1}{2}G_0\bar{u}^2 \quad , \quad (4.10)$$

and after substituting for  $\bar{u}$  and integrating we find that

$$\bar{p} = -\frac{1}{2}G_0 \left[ \frac{1}{5}F^2y^5 - \frac{1}{2}AFy^4 + \frac{1}{3}A^2y^3 \right] + Q(\tilde{z}, \tilde{t}) \quad , \quad (4.11)$$

where  $Q$  is an arbitrary function of  $\tilde{z}$  and  $\tilde{t}$ . Matching with the pressure in the core at  $y_1$  we find that the constant  $c$  is given by

$$c = G_0 \left[ \frac{6}{5}F^2y_1^5 - \frac{3}{2}AFy_1^4 + \frac{1}{3}A^2y_1^3 \right] - 2Q \quad . \quad (4.12)$$

Below the core we find that

$$\bar{p} = -\frac{1}{2}G_0 \left[ \frac{1}{5}F^2y^5 - \frac{1}{2}\bar{a}Fy^4 + \frac{1}{3}(\bar{a}^2 - 2\bar{b}F)y^3 + \bar{a}\bar{b}y^2 + \bar{b}^2y \right] + \bar{c}(\tilde{z}, \tilde{t}) \quad , \quad (4.13)$$

and matching with the pressure in the core at  $y_2$  we get

$$\begin{aligned} \bar{c} = \frac{1}{2}G_0 \left[ \frac{1}{5}F^2y_2^5 - \frac{1}{2}\bar{a}Fy_2^4 + \frac{1}{3}(\bar{a}^2 - 2\bar{b}F)y_2^3 + \bar{a}\bar{b}y_2^2 + \bar{b}^2y_2 - \frac{6}{5}F^2y_1^5 + \frac{3}{2}AFy_1^4 - \frac{1}{3}A^2y_1^3 \right. \\ \left. - y_1y_2(A - y_1F)\{y_2(A - 2y_1F) - y_1(A - 3y_1F)\} \right] + Q \quad . \quad (4.14) \end{aligned}$$

The  $z$ -momentum equation in region IIIb is (2.7d) and integrating twice with respect to  $y$  and using the boundary condition  $\bar{w} = 0$  at  $y = 0$  we obtain

$$\bar{w} = -\frac{1}{2}G_0 \left[ \frac{1}{210}\{F^2\}_{\tilde{z}}y^7 - \frac{1}{60}\{AF\}_{\tilde{z}}y^6 + \frac{1}{60}\{A^2\}_{\tilde{z}}y^5 \right] + \frac{1}{2}Q_{\tilde{z}}y^2 + C(\tilde{z}, \tilde{t})y \quad , \quad (4.15)$$

where  $C$  is another arbitrary function of  $\tilde{z}$  and  $\tilde{t}$ . We know that the position of the upper edge of the core occurs where  $\partial\bar{w}/\partial y = 0$  and this produces the condition

$$0 = -\frac{1}{2}G_0 \left[ \frac{1}{30}\{F^2\}_{\tilde{z}}y_1^6 - \frac{1}{10}\{AF\}_{\tilde{z}}y_1^5 + \frac{1}{12}\{A^2\}_{\tilde{z}}y_1^4 \right] + Q_{\tilde{z}}y_1 + C \quad . \quad (4.16)$$

From matching  $\bar{w}$  at this upper edge of the core we obtain

$$\frac{\Omega}{k} = -\frac{1}{2}G_0 \left[ \frac{1}{210} \{F^2\}_{zy_1^7} - \frac{1}{60} \{AF\}_{zy_1^6} + \frac{1}{60} \{A^2\}_{zy_1^5} \right] + \frac{1}{2}Q_{zy_1^2} + Cy_1 \quad . \quad (4.17)$$

Integrating (2.7d) in region IIIa twice gives

$$\begin{aligned} \bar{w} = -\frac{1}{2}G_0 \left[ \frac{1}{210} \{F^2\}_{zy^7} - \frac{1}{60} \{\bar{a}F\}_{zy^6} + \frac{1}{60} \{\bar{a}^2 - 2\bar{b}F\}_{zy^5} + \frac{1}{12} \{\bar{a}\bar{b}\}_{zy^4} + \frac{1}{6} \{\bar{b}^2\}_{zy^3} \right] \\ + \frac{1}{2}\bar{c}_zy^2 + \bar{d}(z, \tilde{t})y + \bar{e}(z, \tilde{t}) \quad , \quad (4.18) \end{aligned}$$

and matching  $\partial\bar{w}/\partial y$  at  $y_2$  gives

$$\bar{d} = \frac{1}{2}G_0 \left[ \frac{1}{30} \{F^2\}_{zy_2^6} - \frac{1}{10} \{\bar{a}F\}_{zy_2^5} + \frac{1}{12} \{\bar{a}^2 - 2\bar{b}F\}_{zy_2^4} + \frac{1}{3} \{\bar{a}\bar{b}\}_{zy_2^3} + \frac{1}{2} \{\bar{b}^2\}_{zy_2^2} \right] - \bar{c}_{zy_2} \quad , \quad (4.19)$$

whilst matching  $\bar{w}$  gives

$$\begin{aligned} \bar{e} = \frac{\Omega}{k} + \frac{1}{2}G_0 \left[ \frac{1}{210} \{F^2\}_{zy_2^7} - \frac{1}{60} \{\bar{a}F\}_{zy_2^6} + \frac{1}{60} \{\bar{a}^2 - 2\bar{b}F\}_{zy_2^5} \right. \\ \left. + \frac{1}{12} \{\bar{a}\bar{b}\}_{zy_2^4} + \frac{1}{6} \{\bar{b}^2\}_{zy_2^3} \right] - \frac{1}{2}\bar{c}_{zy_2} - \bar{d}y_2 \quad . \quad (4.20) \end{aligned}$$

We must satisfy the boundary condition  $\bar{w} = 0$  at  $y = q$  and from equation (4.18) this implies that

$$\begin{aligned} 0 = -\frac{1}{2}G_0 \left[ \frac{1}{210} \{F^2\}_{zq^7} - \frac{1}{60} \{\bar{a}F\}_{zq^6} + \frac{1}{60} \{\bar{a}^2 - 2\bar{b}F\}_{zq^5} \right. \\ \left. + \frac{1}{12} \{\bar{a}\bar{b}\}_{zq^4} + \frac{1}{6} \{\bar{b}^2\}_{zq^3} \right] + \frac{1}{2}\bar{c}_zq^2 + \bar{d}q + \bar{e} \quad . \quad (4.21) \end{aligned}$$

Finally we need to consider the continuity equation. Above the core we find, after integrating (2.7a) and applying the boundary condition  $\bar{v} = 0$  at  $y = 0$ , that

$$\bar{v} = \frac{1}{2}G_0 \left[ \frac{1}{1680} \{F^2\}_{zzzy^8} - \frac{1}{420} \{\bar{a}F\}_{zzzy^7} + \frac{1}{360} \{A^2\}_{zzzy^6} \right] - \frac{1}{6}Q_{zzzy^3} - \frac{1}{2}C_{zy^2} \quad , \quad (4.22)$$

and matching  $\bar{v}$  at  $y_1$  implies that  $b$  is determined by

$$b = \frac{1}{2}G_0 \left[ \frac{1}{1680} \{F^2\}_{zzzy_1^8} - \frac{1}{420} \{\bar{a}F\}_{zzzy_1^7} + \frac{1}{360} \{A^2\}_{zzzy_1^6} \right] - \frac{1}{6}Q_{zzzy_1^3} - \frac{1}{2}C_{zy_1^2} + \{\Omega/k\}_{zy_1} \quad . \quad (4.23)$$

In region IIIa we again have (2.7a) and after substituting in and integrating once we find that

$$\bar{v} = \frac{1}{2}G_0 \left[ \frac{1}{1680} \{F^2\}_{zzzy^8} - \frac{1}{420} \{\bar{a}F\}_{zzzy^7} + \frac{1}{360} \{\bar{a}^2 - 2\bar{b}F\}_{zzzy^6} + \frac{1}{60} \{\bar{a}\bar{b}\}_{zzzy^5} + \frac{1}{24} \{\bar{b}^2\}_{zzzy^4} \right]$$

$$-\frac{1}{6}\bar{c}_{zz}y^3 - \frac{1}{2}\bar{d}_{zy}y^2 - \bar{e}_{zy} + \bar{f}(\tilde{z}, \tilde{t}) \quad , \quad (4.24)$$

whilst matching with the vertical velocity in the core at  $y_2$  determines  $\bar{f}$ ;

$$\begin{aligned} \bar{f} = & \frac{1}{2}G_0 \left[ \frac{1}{1680}\{F^2\}_{zz}y_1^8 - \frac{1}{420}\{AF\}_{zz}y_1^7 + \frac{1}{360}\{A^2\}_{zz}y_1^6 \right] - \frac{1}{2}G_0 \left[ \frac{1}{1680}\{F^2\}_{zz}y_2^8 - \frac{1}{420}\{\bar{a}F\}_{zz}y_2^7 \right. \\ & \left. + \frac{1}{360}\{\bar{a}^2 - 2\bar{b}F\}_{zz}y_2^6 + \frac{1}{60}\{\bar{a}\bar{b}\}_{zz}y_2^5 + \frac{1}{24}\{\bar{b}^2\}_{zz}y_2^4 \right] + \{\Omega/k\}_z(y_1 - y_2) - \frac{1}{6}Q_{zz}y_1^3 - \frac{1}{2}C_{zy_1}^2 \\ & + \frac{1}{6}\bar{c}_{zz}y_2^3 + \frac{1}{2}\bar{d}_{zy}y_2^2 + \bar{e}_{zy}y_2 \quad . \end{aligned} \quad (4.25)$$

The final boundary condition we have to satisfy from (2.8) is  $\bar{v} = 0$  at  $y = q$  and this implies that

$$\begin{aligned} 0 = & \frac{1}{2}G_0 \left[ \frac{1}{1680}\{F^2\}_{zz} - \frac{1}{420}\{\bar{a}F\}_{zz}q^7 + \frac{1}{360}\{\bar{a}^2 - 2\bar{b}F\}_{zz}q^6 + \frac{1}{60}\{\bar{a}\bar{b}\}_{zz}q^5 + \frac{1}{24}\{\bar{b}^2\}_{zz}q^4 \right] \\ & - \frac{1}{6}\bar{c}_{zz}q^3 - \frac{1}{2}\bar{d}_{zy}q^2 - \bar{e}_{zy}q + \bar{f} \quad . \end{aligned} \quad (4.26)$$

We now have seven equations (4.3, 4.8-9, 4.16-17, 4.21 and 4.26) which relate the eight unknowns ( $A, F, C, Q_{z,y_1}, y_2, \Omega$  and  $k$ ). If we can determine a solution at an initial time location we can then use the phase conservation equation

$$\frac{\partial k}{\partial \tilde{t}} + \frac{\partial \Omega}{\partial \tilde{z}} = 0 \quad , \quad (4.27)$$

to march the solution forwards in time.

## 5 Numerical Solutions

In this section we explain the numerical method used to obtain solutions of the system of equations derived in the last section and we consider results for a variety of different outer channel walls and initial wavenumber distributions,  $k(\tilde{z}, \tilde{t} = 0)$ .

If we rescale  $A, y_1$  and  $y_2$  by writing

$$A = qF\tilde{A} \quad , \quad y_1 = q\tilde{y}_1 \quad , \quad y_2 = q\tilde{y}_2 \quad , \quad (5.1)$$

we find that equations (4.3,8,9) become

$$\begin{aligned} \frac{k^4}{G_0q^3F^2} = & \tilde{y}_1(\tilde{A} - \tilde{y}_1)(\tilde{A} - 2\tilde{y}_1) \quad , \quad (5.2) \\ 0 = & -(1 - \tilde{y}_2)^2 + \frac{(1 - \tilde{y}_2)\tilde{y}_1^{\frac{1}{2}}(\tilde{A} - \tilde{y}_1)^{\frac{1}{2}}(\tilde{A} - 2\tilde{y}_1)}{[2\tilde{y}_2(\tilde{A} - 2\tilde{y}_1) - \tilde{y}_1(\tilde{A} - 3\tilde{y}_1)]^{\frac{1}{2}}} \end{aligned}$$

$$+\tilde{y}_1^{\frac{1}{2}}(\tilde{A}-\tilde{y}_1)^{\frac{1}{2}}[2\tilde{y}_2(\tilde{A}-2\tilde{y}_1)-\tilde{y}_1(\tilde{A}-3\tilde{y}_1)]^{\frac{1}{2}} \quad , \quad (5.3)$$

$$(\tilde{A}-2\tilde{y}_2) = \frac{\tilde{y}_1^{\frac{1}{2}}(\tilde{A}-\tilde{y}_1)^{\frac{1}{2}}(\tilde{A}-2\tilde{y}_1)}{[2\tilde{y}_2(\tilde{A}-2\tilde{y}_1)-\tilde{y}_1(\tilde{A}-3\tilde{y}_1)]^{\frac{1}{2}}} \quad . \quad (5.4)$$

We can introduce the variable  $\eta = k^4/(G_0q^3F^2)$  and then solve for  $\tilde{A}$ ,  $\tilde{y}_1$ ,  $\tilde{y}_2$  and their derivatives numerically. We do this by taking an initial guess at  $\tilde{y}_1$  (for a given  $\eta$ ) so that (5.2) is a quadratic in  $\tilde{A}$ . After solving this we then solve the square of (5.4) which is a cubic for  $\tilde{y}_2$  and substitute our answers into (5.3) to check if we need to iterate on our choice of  $\tilde{y}_1$ . Obviously there are six possible sets of answers but we find that only one set is permissible (both  $\tilde{y}_1$  and  $\tilde{y}_2$  real with  $0 < \tilde{y}_1, \tilde{y}_2 < 1$  and  $\tilde{y}_2 > \tilde{y}_1$ ). We plot  $\tilde{A}$ ,  $\tilde{y}_1$  and  $\tilde{y}_2$  along with their first and second derivatives (as these will be needed for our further calculations) in Figures 2-7. Numerically we find that a solution exists for  $\eta$  greater than zero and less than approximately 0.104. The lower limit corresponds to the core occupying the entire channel and the upper limit occurs when  $\tilde{y}_1$  and  $\tilde{y}_2$  coalesce and the core region disappears. However, we note that there may be some error in the value of this upper limit as the solution becomes extremely difficult to follow numerically in this region because of the rapid changes in the derivatives.

If we know the distribution of  $k$  at an initial time and also  $F$  and its first derivative at some  $\tilde{z}$  location we can use equation (4.21) to determine the unknown  $Q_{\tilde{z}}$ . Upon substitution equation (4.21) becomes

$$Q_{\tilde{z}} = \frac{2}{[(q-y_2)^2 - y_1^2]} \left[ -\frac{G_0}{2} \left[ \frac{1}{210} \{F^2\}_{\tilde{z}} (y_2^6 [7q - 6y_2] - q^7) - \frac{1}{60} \{\bar{a}F\}_{\tilde{z}} (y_2^5 [6q - 5y_2] - q^6) \right. \right. \\ \left. \left. + \frac{1}{60} \{(\bar{a}^2 - 2\bar{b}F)\}_{\tilde{z}} (y_2^4 [5q - 4y_2] - q^5) + \frac{1}{12} \{\bar{a}\bar{b}\}_{\tilde{z}} (y_2^3 [4q - 3y_2] - q^4) + \frac{1}{6} \{\bar{b}^2\}_{\tilde{z}} (y_2^2 [3q - 2y_2] - q^3) \right] \right. \\ \left. - \frac{1}{2} (q - y_2)^2 \tilde{c}_{\tilde{z}} - \frac{G_0}{2} \left[ \frac{1}{35} \{F^2\}_{\tilde{z}} y_1^7 - \frac{1}{12} \{AF\}_{\tilde{z}} y_1^6 + \frac{1}{15} \{A^2\}_{\tilde{z}} y_1^5 \right] \right] \quad , \quad (5.5)$$

where for convenience we have introduced

$$\tilde{c} = \bar{c} - Q \quad . \quad (5.6)$$

We can then determine the unknown  $C$  from (4.16) and the frequency  $\Omega$  from (4.17). Finally after lengthy substitution we can determine the second derivative of  $F$  from the final boundary condition, (4.26), and thus obtain a full solution of our equations at an initial time location. This solution is then marched forward in time by using the phase conservation equation, (4.27). We note that (5.5) implies that a singular solution will occur for  $Q_{\tilde{z}}$  when  $y_1 = (q - y_2)$  but, this only happens when  $\eta = 0$  (see Figure 2) and so will not concern us.

We now consider some specific functions for the outer wall,  $q$ , and determine in particular the effect they have on the vortex wavenumber. For all of these calculations we shall take  $G_0 = 1$  and assume that  $F(\tilde{z} = 0) = 1$ ,  $F_{\tilde{z}}(\tilde{z} = 0) = 0$ . Obviously there is a virtually infinite choice of outer walls and initial wavenumber distributions and our numerical work here only covers a few of these. The particular cases we highlight here are relatively simple ones and have been chosen in an effort to display the effects that individual features have. We have

concentrated on variations in the outer wall as opposed to variations in the distribution of the wavenumber at  $\tilde{t} = 0$  (which we have taken to be constant in all of these cases) because the wall geometries we consider cause the wavenumber distribution to become non-constant anyway. We were also particularly interested in the effect that the geometry of the channel has on the observed wavenumber.

The first case we considered was that where there is a slight increase in the width of the channel. The function  $q$  was defined as

$$q = 1.15 \quad , \quad \tilde{z} < 10.0 \quad \text{and} \quad q = 1.2 - 0.05e^{-(\tilde{z}-10)^3} \quad , \quad \tilde{z} > 10.0 \quad , \quad (5.7)$$

and is shown in Figure 8 along with the extent of the core region for an initial distribution of the wavenumber  $k(\tilde{z}, \tilde{t} = 0) = 0.5$ . In Figure 9 we plot the value of the wavenumber at time intervals of  $\tilde{t} = 125,000$ . The expansion of the channel causes the wavenumber to increase before the expansion and decrease after it. As time passes the effect of the change in the channel width on the wavenumber is felt both further upstream and downstream in the spanwise direction but we note that the wavenumber changes very slowly in time. The changes in the wavenumber are insufficient to produce a change in the core position that would be graphically noticeable on Figure 8. These results plus further unplots and a consideration of  $\partial\Omega/\partial\tilde{z}$  values suggest that the wavenumber eventually settles down to a different steady state.

The second case we considered was that of a constriction of the channel with the function  $q$  now given by

$$q = 1.1 \quad , \quad \tilde{z} < 10.0 \quad \text{and} \quad q = 1.0 + 0.1e^{-(\tilde{z}-10)^3} \quad , \quad \tilde{z} > 10.0 \quad . \quad (5.8)$$

See Figure 10 for a plot of this and the position of the core, where we have again chosen an initial distribution of the wavenumber  $k(\tilde{z}, \tilde{t} = 0) = 0.5$ . In Figure 11 we show the value of the wavenumber at  $\tilde{t} = 125,000$  and  $\tilde{t} = 250,000$  for this case. A constriction of the channel has the opposite effect to an expansion with the wavenumber decreasing before the change in the channel width and increasing afterwards. The other point to be noted from this case is that a larger change in the channel width (0.1 as opposed to 0.05 for the expansion of the channel that we looked at) has produced a larger and quicker change in the wavenumber.

A more interesting case to consider is that where the outer wall of the channel is a periodic function. For this we have considered

$$q = 1.8 \quad , \quad \tilde{z} < 10.0 \quad \text{and} \quad \tilde{z} > 10.0 + 4\pi \quad ,$$

$$q = 1.775 + 0.05 \cos(\tilde{z} - 10) - 0.025 \cos^2(\tilde{z} - 10) \quad , \quad 10.0 < \tilde{z} < 10.0 + 4\pi \quad , \quad (5.9)$$

so that the first and second derivatives of  $q$  are continuous throughout the range of  $\tilde{z}$  that we consider. Figure 12 shows the channel and core position for this wall function and, again, a distribution of  $k = 0.5$  at  $\tilde{t} = 0$ . We note that the top edge of the core is sufficiently close to the wall to not be visible in this graph and also that the position of the core continues to change for values of  $\tilde{z}$  considerably greater than that at which changes to the channel wall stop. The value of  $y_2$ , the lower edge of the core region, eventually settles at about 0.931. In Figure 13 we have plotted the wavenumber at  $\tilde{t} = 4,000$  and  $\tilde{t} = 8,000$ . The wavenumber is again changing

slowly in time and we also note that in the spanwise direction it soon returns to its initial value after the channel wall stops altering. These results bring up the interesting possibility of some complicated wall variation having a small effect on the vortex wavenumber itself (and only close to the position of the variations) but a much larger influence on the vortices through its effect on the position of the core region, maybe even leading to the core region being pinched out of existence at a location some distance downstream (in the spanwise direction) from the changes in the channel geometry.

Further investigations show that the disappearance of vortex activity altogether through the narrowing of the core region is possible but this will probably occur close to the area where the wall alters. If we change the initial distribution of the wavenumber to  $k = 0.70$  we find (see Figure 14) that although we end up with a narrower core region the changes in the position of this core region stop not long after the area of wall variation is passed. Increasing the initial value of the wavenumber further to  $k = 0.7092$  results in the core region of vortex activity being extinguished, Figure 15, but this occurs just after the region where the outer wall is periodic.

## 6 Conclusions

In this paper we have considered the problem of wavenumber selection for small-wavelength Görtler vortices in a curved channel flow. Following an analysis similar to that of Hall & Lakin (1988) but with modifications for the flow being in a curved channel and the vortex wavenumber being dependent on slow spanwise and time scales we have obtained a system of equations which can be solved numerically for the vortex wavenumber. Our results, contained in the previous section, concentrate on the problem where the outer wall of the curved channel varies on the same slow spanwise scale as the phase variable of the vortices. The reasoning behind this was a desire to determine what effect wall geometries could have on the patterns of vortices observed. Alternatively we could have considered the evolution of a system of vortices that started, for our problem, with a non-uniform spanwise wavenumber.

The work in this paper has shown that it is possible to use phase-equation methods to track changes in the wavenumber of Görtler vortices. It would be desirable to extend this to the problem of an external flow where the vortex wavenumber would be dependent on slow time, streamwise and spanwise scales. In particular this would complement other recent studies on Görtler vortices in three-dimensional boundary layers which have been prompted by the development of laminar flow control airfoils with significant areas of concave curvature on the underside of the wing near to the leading edge. Unfortunately it is not possible to consider the current problem in an external boundary layer because the structure of equations (3.1a–d) will not suffice when the phase variable of the vortices is a function of the streamwise variable. So in order to make such an extension it will be necessary to find an alternative system of Görtler vortex equations that is amenable to asymptotic investigation. We note however, that this may be difficult and even for the problem considered in this paper, which is particularly receptive to an asymptotic analysis, we end up with a complicated system of equations; the solution of which requires quite lengthy numerical computations.

The numerical results we have obtained suggest that the vortex wavenumber will respond to variations in the geometry of the outer wall of the channel with small changes occurring over quite large lengths of time. These small changes in the wavenumber cause only minor changes in the other flow quantities as time progresses. However, more dramatic changes in the spanwise direction for the flow outside the core (caused by the variations in the wall) can it appears influence the vortices. It seems that for certain initial conditions and wall variations (see Figure 15) the core region of vortex activity can even be pinched out of existence.

Finally we compare our results with those of experimental studies on Görtler vortex wavelength selection. The large size of our Görtler number makes direct comparison with experimental work difficult but it appears that this choice of Görtler number is required in order to make analytical progress. Our results (see Figures 9, 11 and 13) suggest that changes in the ‘global’ geometry of the channel will produce different vortex patterns but will have very little effect on the average wavenumber (and hence wavelength). This is supported by the work of Swearingen & Blackwelder (1986); one of whose findings was that the average wavelength is independent of the test section spanwise width.

The comparatively small changes to the vortex wavenumber which we have found in this paper show the need for a theoretical investigation of wavenumber selection at the onset of vortex instability in order to explain the large differences in the vortex wavelength which have been obtained in experimental work. It was observed by Tani (1962) and Tani & Sakagami (1964) that the vortex wavelength changed when a different experimental facility was used and it has been possible to alter the observed wavelength by the artificial means of the introduction of disturbances upstream of the onset of vortex activity (see Myose & Blackwelder 1991 for a discussion of the different experiments that have been conducted). However, as pointed out by Myose & Blackwelder (1991) the exact process of wavelength selection is not yet well-understood. Our results here confirm that the initial selection of the wavenumber, at the start of vortex activity, needs theoretical consideration. Unfortunately ‘phase-equation’ methods would appear to be of no use in describing the effects of disturbances that are periodic in the spanwise direction with spacing of the order of the wavelength of the Görtler vortices, as was the case for the experiments of Swearingen & Blackwelder (1986). Once this problem of wavenumber selection near the onset of vortex activity has been tackled the phase-equation method detailed in this paper will allow further changes in the wavenumber to be predicted.

## References

- Bassom, A.P. (1989). On the effect of crossflow on nonlinear Görtler vortices in curved channel flows. *Q. J. Appl. Math.*, **42**, 495-510.
- Buell, J.C. & Catton, I. (1986). Wavenumber selection in ramped Rayleigh–Bénard convection. *J. Fluid Mech.*, **171**, 477-494.
- Cross, M.C. & Newell, A.C. (1984). Convection patterns in large aspect ratio systems. *Physica* **10D**, 299-328.
- Guo, Y. & Finlay, W.F. (1994). Wavenumber selection and irregularity of spatially developing nonlinear Dean and Görtler vortices. *J. Fluid Mech.*, **264**, 1-40.
- Hall, P. (1982). On the Non-linear Evolution of Görtler vortices in Non-parallel Boundary Layers. *J. Inst. Math. Applics.*, **29**, 173-196.
- Hall, P. (1994) A phase equation approach to boundary layer instability theory: Tollmien–Schlichting waves. *ICASE Report No. 94-23 and submitted to J. Fluid Mech.* .
- Hall, P. & Lakin, W.D. (1988). The fully nonlinear development of Görtler vortices in growing boundary layers. *Proc. R. Soc. Lond. A*, **415**, 421-444.
- Hastings, S.P. & McLeod, J.B. (1980). A Boundary Value Problem Associated with the Second Painlevé Transcendent and the Korteweg–de Vries Equation. *Arch. Rational Mech. Anal.*, **73**, 31-51.
- Howard, L.N. & Kopell, N. (1977). Slowly varying waves and shock structures in reaction–diffusion equations. *Stud. Appl. Math.*, **56**, 95-145.
- Kramer, L., Ben–Jacob, E., Brand, H. & Cross, M.C. (1982). Wavelength Selection in Systems Far from Equilibrium. *Phys. Rev. Lett.*, **49**, 1891-1894.
- Myose, R.Y. & Blackwelder, R.F. (1991). Controlling the Spacing of Streamwise Vortices on Concave Walls. *AIAA Journal*, **29**, 11, 1901–1905.
- Newell, A.C., Passot, T. & Lega, J. (1993). Order Parameter Equations for Patterns. *Annu. Rev. Fluid Mech.*, **25**, 399-453.
- Swearingen, J.D. & Blackwelder, R.F. (1986). Spacing of Streamwise Vortices on Concave Walls. *AIAA Journal*, **24**, 10, 1706-1709.
- Swearingen, J.D. & Blackwelder, R.F. (1987). The growth and breakdown of streamwise vor-

tices in the presence of a wall. *J. Fluid Mech.*, **182**, 255-290.

Tani, I. (1962). Production of Longitudinal Vortices in the Boundary Layer Along a Concave Wall. *Journal of Geophysical Research*, **67**, 8, 3075-3080.

Tani, I. & Sakagami, J. (1964). Boundary-Layer Instability at Subsonic Speeds. *Proceedings of the Third Congress of the International Council of Aerospace Sciences, Stockholm 1962*, Spartan, Washington DC, 391-403.

Whitham, G.B. (1974). *Linear and Nonlinear Waves*. New York: Wiley-Interscience.

Figure 1. A schematic picture of the different regions of the flow in the curved channel.



Figure 2. The functions  $\tilde{y}_1$  and  $\tilde{y}_2$  which determine the boundaries of the core.

$y$

Figure 3. The first derivatives of  $\tilde{y}_1$  and  $\tilde{y}_2$ .

$dy/d\eta$

Figure 4. The second derivatives of  $\tilde{y}_1$  and  $\tilde{y}_2$ .

$$d^2y/d\eta^2$$

Figure 5. The function  $\tilde{A}$ .

$$A$$

Figure 6. The first derivative of  $\tilde{A}$ .

$$dA/d\eta$$

Figure 7. The second derivative of  $\tilde{A}$ .

$$d^2A/d\eta^2$$

Figure 8. The function  $q$  from equation (5.7).

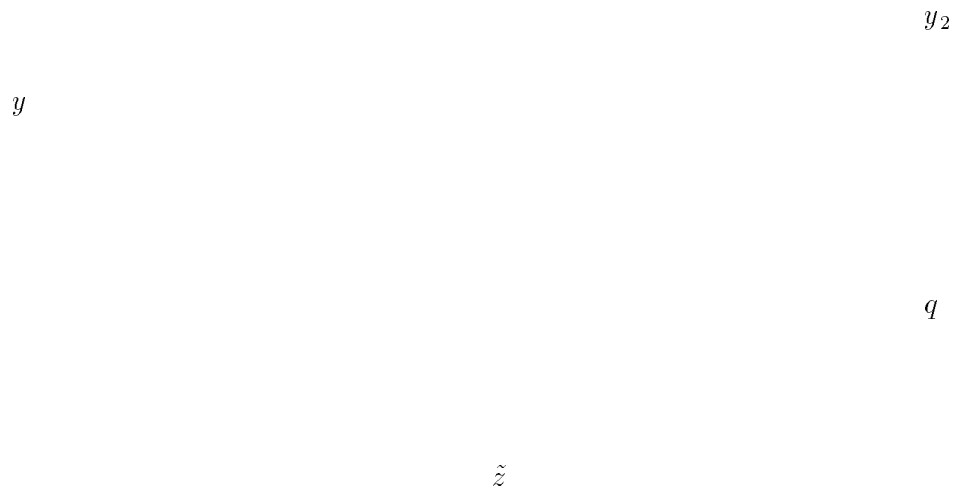


Figure 9. The wavenumber,  $k$ , for the channel given by  $q$  from (5.7).

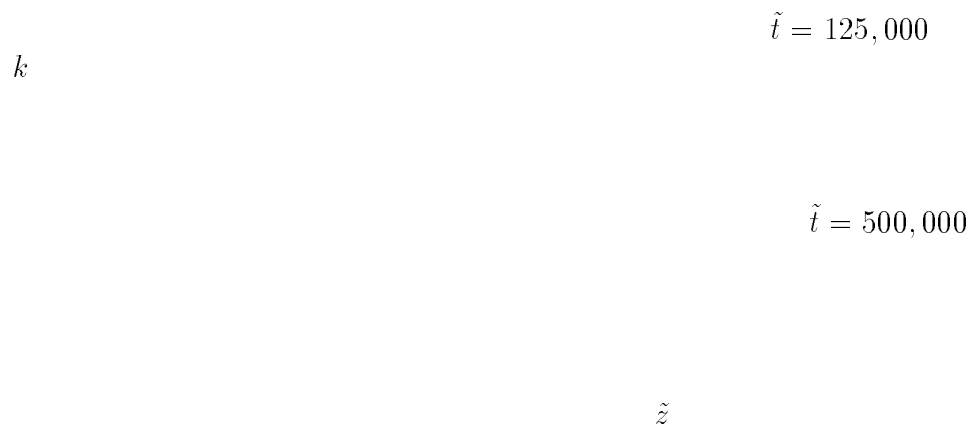


Figure 10. The function  $q$  from equation (5.8).

$y$

$\tilde{z}$

Figure 11. The wavenumber,  $k$ , for the channel given by  $q$  from (5.8).

$k$

$\tilde{t} = 250,000$

$\tilde{t} = 125,000$

$\tilde{z}$

Figure 12. The function  $q$  from equation (5.9).

$y$

$\tilde{z}$

Figure 13. The wavenumber,  $k$ , for the channel given by  $q$  from (5.9).

$k$

$\tilde{z}$

Figure 14. The core region with  $q$  from (5.9) and  $k(\tilde{t} = 0) = 0.70$ .

$y$

$\tilde{z}$

Figure 15. The core region with  $q$  from (5.9) and  $k(\tilde{t} = 0) = 0.7092$ .

$y_1$

$y_2$

$y$

$q$

$\tilde{z}$